International Immunopharmacology 75 (2019) 105563

Contents lists available at ScienceDirect

International Immunopharmacology

journal homepage: www.elsevier.com/locate/intimp

Protective effects of Clematichinenoside AR against inflammation and cytotoxicity induced by human tumor necrosis factor-α

Ying Xiong[a,b], Yan Ma[a], Nandani Darshika Kodithuwakku[d], Weirong Fang[a], Lifang Liu[e], Fengwen Li[f], Yahui Hu[a,c,*], Yunman Li[a,*]

[a] State Key Laboratory of Natural Medicines, Department of Physiology, China Pharmaceutical University, # 24 TongJiaXiang, Nanjing 210009, PR China
[b] Department of Pharmacology, Wannan Medical College, # 22 WenChang West Road, Wuhu 241002, PR China
[c] Department of Pharmacy, Children's Hospital of Nanjing Medical University, # 72 GuangZhou Road, Nanjing 210008, PR China
[d] Institute of Indigenous Medicine, University of Colombo, Rajagiriya 11600, Sri Lanka
[e] State Key Laboratory of Natural Medicines, Department of Chinese Medicines Analysis, China Pharmaceutical University, # 24 TongJiaXiang, Nanjing 210009, PR China
[f] Department of Traditional Chinese Pharmacy, China Pharmaceutical University, # 24 TongJiaXiang, Nanjing 210009, PR China

ARTICLE INFO

Keywords:
Clematichinenoside AR
Protective effects
Human tumor necrosis factor-α
Inflammation
Cytotoxicity

ABSTRACT

Clematichinenoside AR (AR), a major active ingredient extracted from traditional Chinese herb *Clematis chinensis* Osbeck, has been demonstrated to possess anti-inflammatory and immune-modulatory activities in the treatment of experimental rheumatoid arthritis (RA). The therapeutic potential of AR was supposed to be closely correlated to its ability against tumor necrosis factor-α (TNF-α). Therefore, we aimed to explore the protective effects of Clematichinenoside AR against inflammation and cytotoxicity induced by human TNF-α. AR treatment significantly decreased IL-6 and IL-8 secretion, and attenuated MMP-1 production in human RA-derived fibroblast-like synoviocyte MH7A cells stimulated by recombinant human TNF-α (rhTNF-α). AR might antagonize rhTNF-α-induced responses in MH7A cells through inhibiting p38 and ERK MAPKs signal activation. In TNF-α-sensitive murine fibroblast L929 cells, AR treatment attenuated the proliferation inhibition ratio induced by rhTNF-α/ActD and antagonized rhTNF-α-induced cytotoxicity. The cellular and nuclear morphological alterations in apoptotic characteristics induced by rhTNF-α/ActD in L929 cells were observed to be attenuated by the pretreatment with AR under a phase-contrast and fluorescence microscopy, respectively. The Annexin V-FITC/PI double-staining assay was performed to confirm that AR pretreatment obviously decreased the cell death. The antagonistic effects of AR against rhTNF-α-induced cytotoxicity might be potentially attributed to the degeneration of reactive oxygen species and the increasing of mitochondrial membrane potential, along with the suppression of durative phosphorylation of c-Jun N-terminal kinase (JNK). Collectively, our results indicated that AR antagonizes the inflammatory and cytotoxic activities induced by human TNF-α effectively *in vitro*, which provided further evidence for a novel mechanism underlying AR for treating RA correlating with excessive TNF-α production.

1. Introduction

Clematis chinensis Osbeck, a traditional Chinese herb, has been used widely in the treatment of autoimmune and inflammatory diseases. Clematichinenoside AR (AR) has been defined as the major active ingredient of triterpenoid saponins extracted from the roots of *Clematis chinensis* Osbeck. Recent studies have been demonstrated that AR is remarkably effective in controlling inflammation and modulating

Abbreviations: ActD, Actinomycin D; AR, Clematichinenoside AR; DCF, dichlorofluorescein; DCFH-DA, 2′,7′-dichloro-dihydrofluorescein diacetate; DMEM, Dulbecco's modified Eagle's medium; ELISA, Enzyme-linked immunosorbent assay; ERK, extracellular signal-regulated kinase; FBS, fetal bovine serum; FLSs, fibroblast-like synoviocytes; JC-1, 5,5′,6,6′-tetrachloro-1,1′,3,3′-tetraethyl-imidacarbocyanine iodide; JNK, c-Jun N-terminal kinase; MAPKs, mitogen-activated protein kinases; MMPs, matrix metalloproteinases; IL-6, interleukin-6; IL-8, interleukin-8; MTT, 3-(4,5-dimethylthiazol-2-yl)-2,5-diphenyltetrazolium bromide; RA, rheumatoid arthritis; rhTNF-α, recombinant human TNF-α; ROS, reactive oxygen species; TNF-α, tumor necrosis factor-α; TNFR, tumor necrosis factor receptor; Δψm, mitochondrial membrane potential

* Corresponding authors at: Y. Hu, Department of Pharmacy, Children's Hospital of Nanjing Medical University, # 72 GuangZhou Road, Nanjing 210008, PR China; Y. L, State Key Laboratory of Natural Medicines, Department of Physiology, China Pharmaceutical University, #24 TongJiaXiang, Nanjing 210009, PR China
E-mail addresses: huyahui324@163.com (Y. Hu), yunmanlicpu@163.com (Y. Li).

https://doi.org/10.1016/j.intimp.2019.04.010
Received 14 April 2018; Received in revised form 31 March 2019; Accepted 4 April 2019
Available online 10 August 2019

immune reaction, which is beneficial in preventing experimental rheumatoid arthritis (RA) [1–3]. RA is a systemic immune-inflammatory disease characterized by persistent erosive synovitis which leads to structural joint damage and lifelong disability. Abundant pro-inflammatory cytokines that participate in the pathogenesis of RA have been well recognized, among which tumor necrosis factor-α (TNF-α) has been emerged as a pivotal player in the initiation and perpetuation of RA [4,5].

TNF-α is a pleiotropic cytokine participating in diverse cellular responses such as cell proliferation, differentiation, survival and death. As the key inflammatory cytokine produced during various stages in RA, TNF-α in turn contributes to the induction of inflammatory responses through the up-regulation of pro-inflammatory and pro-destructive mediators [6,7]. It has been demonstrated that TNF-α recruits immune and inflammatory cells from the circulation into joints, stimulates synoviocytes activation, and promotes osteoclastogenesis, eventually results in cartilage destruction and bone erosion [8–12]. The anti-TNF-α therapies targeting human TNF-α neutralization or human TNF-α receptor blockade, have been proven to be highly efficacious in improving arthritic symptoms of RA patients [13]. Unexpectedly, clinically available anti-TNF-α biologics including monoclonal antibodies against TNF-α and recombinant soluble TNF-receptor Fc fusion proteins might elicit the formation of anti-drug antibodies due to their immunogenicity which result in the loss of clinical efficacy, and induce serious adverse effects associated with immune imbalance [14–17]. Consequently, there remains a clear medical need for the development of new compounds that target human TNF-α so as to avoid or at least to limit the risks caused by anti-TNF-α biologics.

Based on our previous studies, it has been supposed that the therapeutic potential of AR might be closely correlated to the antagonistic effects against TNF-α. The expressions of TNF-α in the synovial tissue of rats with collagen-induced arthritis (CIA) were obviously reduced by AR administration [3]. The levels of TNF-α in the culture supernatants of ConA-activated lymphocytes isolated from Peyer's Patches as well as in the peripheral blood in rats with adjuvant-induced arthritis (AIA) were significantly inhibited by AR treatment [18]. Moreover, the TNF-α-induced adhesion of monocytes to HUVECs was also inhibited by AR treatment through blocking ROS-dependent NF-κB activity [19]. Hence, it was deserved to further investigate the antagonistic effects of AR against human TNF-α.

Joint resident fibroblast-like synoviocytes (FLSs), the major components of hyperplastic synovial pannus, are capable to secrete synovial fluid and produce cytokines, chemokines as well as matrix-degrading enzymes, resulting in chronic inflammatory state and joint damage in RA [7]. The immortalized human rheumatoid FLS cell line MH7A, which was established by stably transfecting RA FLSs with SV40 T antigen gene [20], was then used to evaluate the effects of AR against inflammatory responses induced by human TNF-α. The murine fibroblast L929 cell line, which is considered to be highly sensitive to TNF-α, has been extensively used in measuring the neutralization activity of TNF-α blockers [21,22]. We therefore utilized L929 cell line to investigate whether AR could antagonize cytotoxic effects induced by human TNF-α, which was combined with low concentration of Actinomycin D (ActD) enabling to increase the susceptibility of L929 cells to TNF-α [23]. Taken together with our previous studies involving the therapeutic potential of AR, the present investigation was aimed to provide a novel mechanistic understanding of the protective effects of AR against inflammation and cytotoxicity induced by human TNF-α.

2. Materials and methods

2.1. Drugs and reagents

AR, which was provided by Jiangsu Chia-tai Tianqing Pharmaceutical Co., Ltd. (Nanjing, China), was suspended and then diluted with serum-free cell culture medium to obtain corresponding concentrations. Dulbecco's Modified Eagle's Medium (DMEM) was the product of Gibco. Recombinant human TNF-α (rhTNF-α) protein was purchased from PeproTech, Inc. (Rocky Hill, NJ, USA). Actinomycin D (ActD) and 3-(4,5-dimethylthiazol-2-yl)-2,5-diphenyltetrazolium bromide (MTT) were purchased from Sigma-Aldrich, Inc. (Saint Louis, MO, USA). Enzyme-linked immunosorbent assay (ELISA) kits for human interleukin-6 (IL-6), interleukin-8 (IL-8), and total matrix metalloproteinase-3 (MMP-3) quantification were purchased from Dakewe Biotech Co., Ltd. (Shenzhen, Guangdong, CN). ELISA kit for human matrix metalloproteinase-1 (MMP-1) was purchased from MultiSciences Biotech Co., Ltd. (Hangzhou, Zhejiang, CN). Hoechst Staining Kit, Reactive Oxygen Species Assay Kit, Mitochondrial Membrane Potential Assay Kit with 5,5′,6,6′-tetrachloro-1,1′,3,3′-tetraethyl-imidacarbocyanine iodide (JC-1), and BCA Protein Assay Kit were purchased from Beyotime Institute of Biotechnology (Haimen, Jiangsu, CN). Annexin V Apoptosis Detection Kit FITC was purchased from eBioscience, Inc. (San Diego, CA, USA). Antibodies against phospho-p38 MAPK (Thr180/Tyr182), p38 MAPK, phospho-ERK1/2 (Thr202/Tyr204) and ERK1/2 were purchased from Cell signaling Technology, Inc. (Danvers, MA, USA). Antibodies against phospho-JNK (Thr183/Tyr185) and JNK were purchased from Bioworld Technology, Inc. (Louis Park, MN, USA). All Other reagents used were of analytical grade from commercial sources.

2.2. Cell culture

The human RA-derived fibroblast-like synoviocyte cell line MH7A was obtained from Guangzhou Jennio Biotech Co., Ltd. (Guangzhou, China). The TNF-α-sensitive mouse fibroblast L929 cell line (CCL-1, ATCC) was obtained from the Cell Resource Center of Shanghai Institutes for Biological Sciences, Chinese Academy of Sciences (Shanghai, China). Cells were maintained in DMEM supplemented with 10% fetal bovine serum (FBS), 100 U/ml penicillin and 100 μg/ml streptomycin at 37 °C in a humidified 5% CO_2 atmosphere.

2.3. ELISA assay to determinate the levels of cytokines secretion

MH7A cells were seeded in flat-bottomed 24-well culture plates at a density of 2×10^4 cells/well. The cells were pre-incubated with different concentrations of AR (3, 10, and 30 μM) for 1 h, followed by exposure simultaneously to rhTNF-α (10 ng/ml) for another 24 h. Following treatment, the cell culture supernatants were collected, and the secretion levels of IL-6, IL-8, MMP-1 and MMP-3 were determined using ELISA kits according to the manufacturer's protocol. Optical densities at 450 nm were measured by a microplate reader, and then the values were calculated on the basis of standard curves.

2.4. MTT assay to detect rhTNF-α mediated cytotoxicity

The inhibition of the cytotoxic effect of rhTNF-α by AR was assessed by the MTT colorimetric assay. L929 cells were seeded at an initial density of 2×10^4 cells/well into 96-well flat-bottomed plates and allowed to attach and grow for 24 h in DMEM containing 10% FBS, then were incubated in serum-free culture medium for 12 h to make them relatively non-proliferated. Thereafter, the culture medium was replaced with fresh culture medium containing 2% FBS, and the cells were incubated with various concentrations of AR (1, 10, and 100 μM) for 1 h, followed by stimulation with TNF-α (5 ng/ml) in the presence of ActD (0.5 μg/ml) for a further 20 h, of which the total volume was 100 μl. Subsequently, 10 μl of MTT in PBS (5 mg/ml) was added into each well and the incubation was continued for a further 4 h. Then 100 μl of triplet solution (10% SDS, 5% isobutanol, 0.012 mol/l HCl) was added to dissolve formazan crystals. The absorbance values at 570 nm were determined using a model 680 microplate reader (Bio-Rad). The inhibition ratio (%) was calculated as follows: Inhibitory ratio (%) = $(1 - OD_{treatment}/OD_{control}) \times 100$. The percentage inhibition of AR against rhTNF-α cytotoxicity was calculated using the

following formula [21,24,25]:

$$\frac{OD_{ActD+TNF-\alpha+AR} - OD_{ActD+TNF-\alpha}}{OD_{ActD} - OD_{ActD+TNF-\alpha}} \times 100$$

2.5. Hoechst 33258 fluorescence staining to observe cellular and nuclear morphological changes

L929 cells were plated in 12-well culture plates at a density of 2×10^5 cells/well for 24 h and incubated in serum-free culture medium for another 12 h. Then the cells were pretreated with different concentrations of AR for 1 h, followed by concurrent exposure to TNF-α (5 ng/ml) in the presence of ActD (0.5 μg/ml) for 24 h. Afterwards, the cells were immersed in fixative solution overnight at 4 °C. Following being washed twice with PBS, the cells were stained with Hoechst 33258 staining solution for 5 min. The solution was then removed and the cells were washed twice again with PBS. The cellular and nuclear morphologies were observed and photographed under a phase-contrast and fluorescence microscope, respectively.

2.6. Annexin V-FITC/PI double-staining assay to detect cell apoptosis/necrosis

To determine the proportion of apoptotic and necrotic cells, L929 cells were double-stained using an Annexin V-FITC/PI apoptosis detection kit. Briefly, L929 cells were seeded in 6-well culture plates at a density of 4×10^5 cells/well for 24 h and incubated in serum-free culture medium for 12 h. The cells were pre-incubated with AR at different concentrations for 1 h, then exposed to TNF-α (5 ng/ml) in the presence of ActD (0.5 μg/ml) for another 24 h. After treatment, both adherent and suspended cells were collected, washed with PBS and binding buffer successively, and then re-suspended in binding buffer. Cells were stained with FITC-labeled Annexin V for 15 min in the dark at room temperature. After being washed, cells were re-suspended and subsequently incubated with propidium iodide (PI) staining solution in the dark. The fluorescent intensity of Annexin V and PI were detected by FACSCalibur flow cytometer (BD Bioscience). The extent of apoptosis was quantified as the percentage of Annexin V-positive cells.

2.7. DCFH-DA staining method to determine the generation of intracellular reactive oxygen species (ROS)

The intracellular ROS levels were determined using the fluorescent probe 2′,7′-dichloro-dihydrofluorescein diacetate (DCFH-DA). Briefly, L929 cells were seeded in 6-well culture plates for 24 h and then incubated in serum-free culture medium for 12 h. The cells were pre-incubated with various concentrations of AR for 1 h prior to the concurrent treatment with TNF-α (5 ng/ml) in the presence of ActD (0.5 μg/ml) for a further 12 h. Both adherent and suspended cells were collected and rinsed in PBS, then incubated with 10 μM DCFH-DA diluted in serum-free culture medium at 37 °C for 20 min. After washing thrice with serum-free medium, the cells were suspended in PBS and immediately subjected to flow cytometry. The fluorescence intensity of dichlorofluorescein (DCF) which is proportional to the amount of ROS produced intracellularly was then detected.

2.8. JC-1 staining assay to analyze mitochondrial membrane potential (Δψm)

The change of Δψm, which acts a reliable parameter of mitochondrial function as well as cell health, was monitored using the dual-emission potential-sensitive probe JC-1. After the treatment as described above, the harvested cells were washed and suspended in serum-free culture medium, evenly blended with JC-1 staining working solution which was prepared following the manufacturer's instruction, and then incubated for 20 min in 5% CO_2 at 37 °C. Stained cells were rinsed twice and finally re-suspended in JC-1 staining buffer. The ratio of red to green fluorescence intensity which indicates the change of Δψm was detected immediately by flow cytometry.

2.9. Western blot analysis to detect the activation of p38, ERK and JNK

After treating, the harvested cells were lysed in ice-cold lysis buffer containing protease and phosphatase inhibitors. The concentrations of total protein obtained were quantified utilizing BCA protein assay. Equivalent amounts of denatured protein samples were separated by sodium dodecyl sulfate-polyacrylamide gel electrophoresis (SDS-PAGE). Separated proteins were transferred onto polyvinylidene difluoride (PVDF) membranes electrophoretically. Following blocking in Tris-buffered saline with Tween-20 (TBST) containing 5% bovine serum albumin or nonfat milk, the membranes were probed with primary antibodies for detecting p38, p-p38, p-ERK, ERK, p-JNK, JNK (dilution 1:1000 or 1:2000) overnight at 4 °C. The membranes were washed thrice and incubated with horseradish peroxidase-conjugated secondary antibodies for 2 h at room temperature. After washing, immunoreactive bands were visualized using the enhanced chemiluminescence method.

2.10. Statistical analysis

All experimental data were shown as mean ± standard deviations (SD). Intergroup comparisons were performed using one-way ANOVA followed by SNK test or Dunnett's T3 test as post hoc analysis, for equal variances assumed or not assumed, respectively. Differences were considered statistically significant when $P < 0.05$.

3. Results

3.1. AR down-regulates the secretion levels of IL-6 and IL-8 induced by rhTNF-α in MH7A cells

The levels of pro-inflammatory cytokines secreted into the culture medium were measured so as to assess the anti-inflammatory activity of

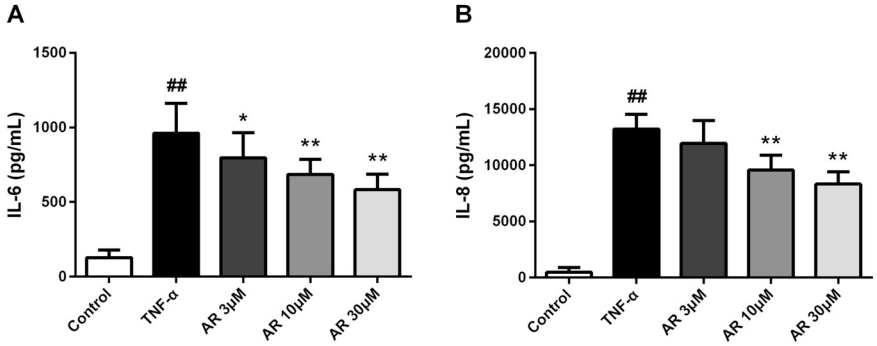

Fig. 1. Effects of AR on the production of pro-inflammatory cytokines induced by rhTNF-α in human RA synovial MH7A cells. The cells were pretreated with various concentrations of AR for 1 h followed by rhTNF-α stimulation for 24 h. The levels of IL-6 and IL-8 in the cell-free culture supernatants were measured by ELISA assay. Data are presented as the mean ± SD of six independent experiments. $^{\#\#}P < 0.01$ versus non-stimulated control group, $^{*}P < 0.05$, $^{**}P < 0.01$ versus rhTNF-α-stimulated group.

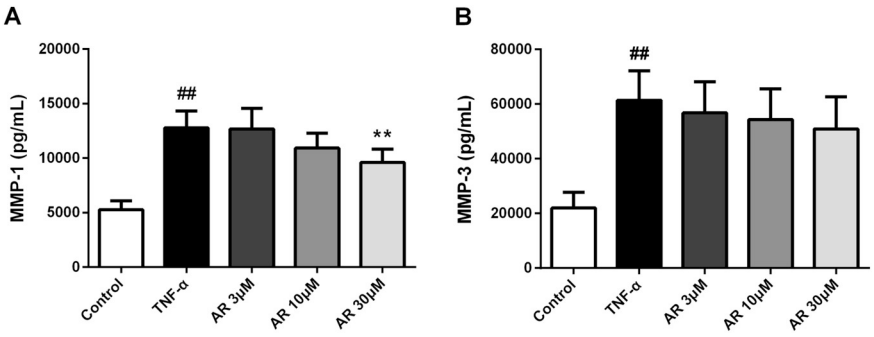

Fig. 2. Effects of AR on the production of pro-destructive mediators induced by rhTNF-α in MH7A cells. The cells were pre-incubated for 1 h with various concentrations of AR followed by rhTNF-α stimulation for 24 h. Protein expressions of MMP-1 and MMP-3 were then analyzed by ELISA assay. Data are presented as the mean ± SD of six independent experiments. $^{\#\#}P < 0.01$ versus non-stimulated control group, $^{**}P < 0.01$ versus rhTNF-α-stimulated group.

AR in rhTNF-α-stimulated synovial MH7A cells. As shown in Fig. 1, exposure of MH7A cells to rhTNF-α resulted in an obvious enhancement of IL-6 secretion, which was reduced significantly by the pretreatment with different concentrations of AR in a concentration-dependent manner. This was accompanied by the obvious enhancement of IL-8 secretion from rhTNF-α-stimulated MH7A cells. Pretreatment with AR concentration-dependently showed a significant reduction of IL-8 production.

3.2. AR inhibits the production of MMP-1 but not MMP-3 induced by rhTNF-α in MH7A cells

Considering the aggressive phenotype of RA FLSs is featured by the increasing expression of matrix metalloproteinases (MMPs), the role of AR in regulating MMPs expression was then detected in rhTNF-α-stimulated MH7A cells. As shown in Fig. 2, MMP1 and MMP-3 were present in the culture supernatants before stimulated with rhTNF-α, but both were notably increased in response to rhTNF-α. AR pretreatment reduced the secretion level of MMP-1 induced by rhTNF-α, of which the highest concentration (30 μM) was most effective. However, no significant decrease of MMP-3 secretion from MH7A cells was observed following AR pretreatment.

3.3. AR inhibits p38 and ERK phosphorylation induced by rhTNF-α in MH7A cells

To determine the signaling molecules associated with AR-mediated rhTNF-α inducing responses in synovial MH7A cells, we assessed phosphorylated mitogen-activated protein kinases (MAPKs) pathways induced by rhTNF-α using western blot analysis. As shown in Fig. 3, the phosphorylated levels of p38 and ERK1/2 were obviously elevated in response to the stimulation of rhTNF-α in MH7A cells when compared with that of unstimulated group, indicating the activation of MAPKs pathway. However, AR pretreatment significantly inhibited the phosphorylated levels of p38 and ERK1/2 induced by rhTNF-α.

3.4. AR suppresses rhTNF-α-induced cytotoxicity in L929 cells

MTT assay was employed to evaluate the inhibitory effects of AR against rhTNF-α-induced cytotoxicity in L929 cells. As shown in Fig. 4A, the inhibition ratio of L929 cell viability reached (55.39 ± 5.60) % in response to rhTNF-α combined with ActD, whereas decreased cell viability due to rhTNF-α/ActD stimulation was significantly ameliorated by AR pretreatment in a concentration-dependent manner. In addition, the inhibition percentage of AR at 100 μM against rhTNF-α cytotoxicity was calculated to be (27.10 ± 6.65) % as indicated in Fig. 4B.

3.5. AR ameliorates L929 cell morphological alterations induced by rhTNF-α in the presence of ActD

The cellular and nuclear morphological features of L929 cells were observed microscopically following Hoechst 33258 fluorescence staining. As shown in Fig. 5, the healthy and regular morphologies of viable L929 cells were observed, in which the uniformly intact nuclei with well-distributed blue fluorescence were exhibited by Hoechst 33258 staining. However, exposure of L929 cells to rhTNF-α plus ActD resulted in a significantly decreased cell density and clear apoptotic characteristics such as irregular cell outline, cytoplasmic shrinkage, condensed or fragmented nuclei with brilliant blue staining. Pretreatment with different concentrations of AR gradually attenuated the cellular damage in a dose-dependent manner. As the cell density increased, the percentage of cells with apoptotic morphologies decreased significantly. These results suggested that AR effectively improve the morphological alterations in L929 cells induced by rhTNF-α in the presence of ActD.

3.6. AR inhibits L929 cellular death induced by rhTNF-α in the presence of ActD

Annexin V-FITC and PI double staining by the flow cytometric

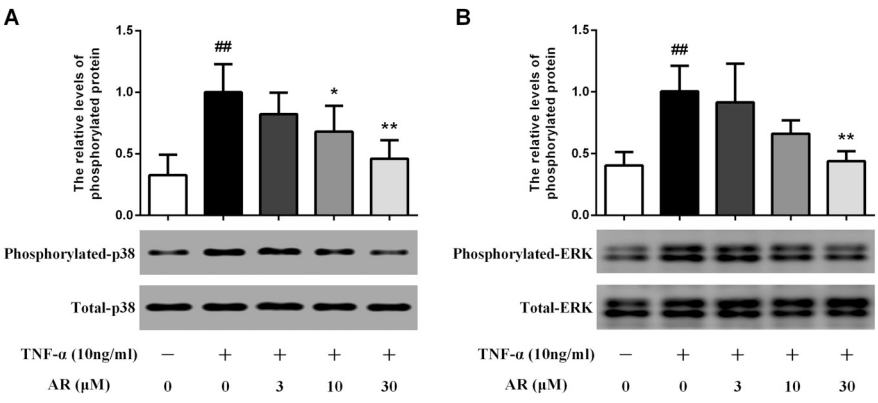

Fig. 3. Influence of AR on the rhTNF-α signal transduction in MH7A cells. MH7A cells were seeded onto 6-well plates at a density of 2×10^5 cells/well and cultured until the cell density reached >80% confluence. MH7A cells were pretreated with or without AR for 24 h, followed by rhTNF (10 ng/ml) stimulation for 15 min. Phosphorylated levels of p38 MAPK and ERK1/2 induced by rhTNF-α were analyzed by western blot analysis. Representative immunoblots are presented, together with the respective densitometric analysis of the p-p38/p38 and p-ERK/ERK ratios. (A) p-p38 MAPK (Thr180/Tyr182) and total p38 MAPK. (B) p-ERK1/2 (Thr202/Tyr204) and total ERK1/2. Data are presented as the mean ± SD of six independent experiments. $^{\#\#}P < 0.01$ versus non-stimulated control group, $^{*}P < 0.05$, $^{**}P < 0.01$ versus rhTNF-α-stimulated group.

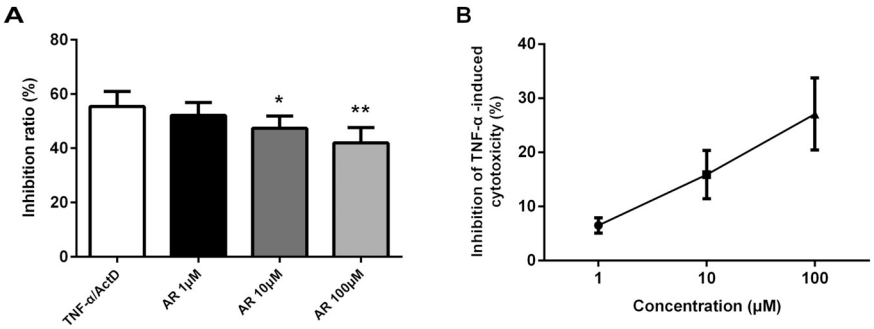

Fig. 4. Effects of AR at different concentrations on cell viability in L929 cells exposed to rhTNF-α (5 ng/ml) in the presence of ActD (0.5 μg/ml) for 24 h. Cell viability was tested using MTT method, and then (A) the inhibition ratio (%) relative to the control group and (B) the percentage inhibition of AR against rhTNF-α cytotoxicity were calculated. Data are presented as the mean ± SD (n = 6). *P < 0.05, **P < 0.01 versus TNF-α/ActD group.

analysis was further employed to quantitatively determine the cell apoptosis/necrosis induced by rhTNF-α. As shown in Fig. 6, exposure to rhTNF-α in the presence of ActD resulted in a significant increase of apoptotic ratio of L929 cells than that observed in the control. Nevertheless, the percentage of Annexin V-positive cells was found to be significantly inhibited by the pre-incubation with different concentrations of AR compared with the rhTNF-α/ActD-induced group.

3.7. AR decreases intracellular accumulation of ROS induced by rhTNF-α in the presence of ActD in L929 cells

Since apoptotic pathway may be triggered through ROS generation, we assessed ROS production utilizing the oxidant sensitive probe. DCFH-DA readily diffuses into the cells, where it is hydrolyzed by intracellular esterase yielding polarized DCFH, and thereby is subsequently oxidized to the fluorescent compound DCF in the presence of ROS. Therefore, we referred to the amount of DCF as the measurement of ROS formed intracellularly. As shown in Fig. 7, following 12 h exposure to rhTNF-α in combination with ActD, there was a significant increase in the level of intracellular ROS production in L929 cells, as detected by flow cytometric assay. When compared with the rhTNF-α/ActD-induced group, the intracellular ROS levels were significantly attenuated in the L929 cells by AR pretreatment.

3.8. AR prevents the decline of Δψm induced by rhTNF-α in the presence of ActD in L929 cells

Considering that the decline of Δψm is a sensitive indicator of mitochondrial functionality damage, JC-1, which exhibits potential-dependent accumulation in mitochondria, was then used for determination. Due to high Δψm in healthy cells, JC-1 selectively accumulates into mitochondrial matrix to form the polymers (JC-1 aggregates) which produce bright red fluorescence. However, at low Δψm in unhealthy cells, JC-1 cannot gather within the mitochondria and remain in the cytoplasm as the monomeric form (JC-1 monomers) emitting green fluorescence. Hence, the decline of Δψm should be indicated by a decrease in the ratio of red fluorescence to green fluorescence. The results presented in Fig. 8. showed that rhTNF-α in the presence of ActD caused a significant reduction in the ratio of red/green fluorescent intensity compared with control group, indicating the level of Δψm was declined due to the dysfunction of mitochondria induced by rhTNF-α in the presence of ActD. However, the decrease in the ratio of red/green fluorescent intensity was significantly enhanced by the pretreatment with AR, demonstrating that AR treatment led to an augmentation of Δψm as the consequence of mitochondrial function stabilization.

3.9. AR suppresses sustained JNK phosphorylation induced by rhTNF-α in the presence of ActD in L929 cells

As shown in Fig. 9, western blot analysis revealed that rhTNF-α/ActD induced the phosphorylation of JNK which indicates JNK activation. When treated with AR, the JNK activation was attenuated obviously at 360 min in L929 cells induced by rhTNF-α in the presence of ActD. Thus, rhTNF-α/ActD-induced cell death is probably mediated by JNK phosphorylation, and AR might exert its protective effects through the inhibition of JNK sustained activation.

4. Discussion

TNF-α, which is overexpressed within rheumatoid synovial tissues and fluid, plays a central role in the pathogenesis of RA [26,27]. Since human TNF-α is closely associated with the activity and severity of RA, it has been validated as a drug target for RA therapy. However, due to the undesirable side effects of biologic-based agents against human TNF-α in RA therapy, more attention has been drawn on the explorations of new drugs with high efficacy and less toxicity as alternative treatments [28]. As the major active compound derived from traditional Chinese medicine, AR has been demonstrated to possesses anti-arthritic potency, which has been proposed to be highly relevant to the blockade of TNF-α.

Accumulating evidences suggest that TNF-α overexpression at the site of inflammation in turn increases the induction of inflammatory cytokines, and promotes the recruitment and activation of inflammatory cells in RA. In this study, the secretion levels of IL-6 and IL-8 were markedly elevated from MH7A cells upon TNF-α stimulation, which indicated that the inflammatory cellular model of human RA FLS had been successfully established. We found that AR treatment significantly inhibited IL-6 and IL-8 release from TNF-α-stimulated MH7A cells, suggesting that AR might prevent inflammatory responses against rhTNF-α by reducing the pro-inflammatory cytokines secretion, therefore dampen the vicious cycle of inflammation.

MMPs, mainly produced by FLSs in RA, are largely responsible for extracellular matrix degradation, which facilitates FLSs migration and invasion, resulting in cartilage and bone destruction [29,30]. Therefore, we investigated the change in critical tissue degradation proteases such as MMP-1 and MMP-3 under AR interference. We found that MMP-1 and MMP-3 were increased markedly upon the stimulation of rhTNF-α in synovial MH7A cells. AR treatment led to a decrease in MMP-1 secretion from rhTNF-α-stimulated MH7A cells, whereas exhibited no inhibitory effect of MMP-3 secretion, indicating that AR might exert anti-destructive effects triggered by rhTNF-α predominantly through down-regulating MMP-1 expression.

The cellular biological processes induced by TNF-α stimulation are mediated by a set of intracellular signaling cascades involving MAPKs, which are important signals involved in modulating synovial inflammation and joint destruction in RA [31,32]. It has been well documented that p38 and extracellular signal-regulated kinase (ERK) MAPK in synovial membrane are preferentially activated upon the exposure to TNF-α [33], and activation of MAPK cascades and pro-inflammatory/pro-destructive features by TNF-α is predominantly mediated by tumor necrosis factor receptor-1 (TNF-R1) in early-passage RA synovial fibroblasts [34]. The p38 and ERK MAPK modulate inflammatory cytokines synthesis and synovial invasion, whereas inhibition of signaling pathways through TNF-α-MAPKs is required to

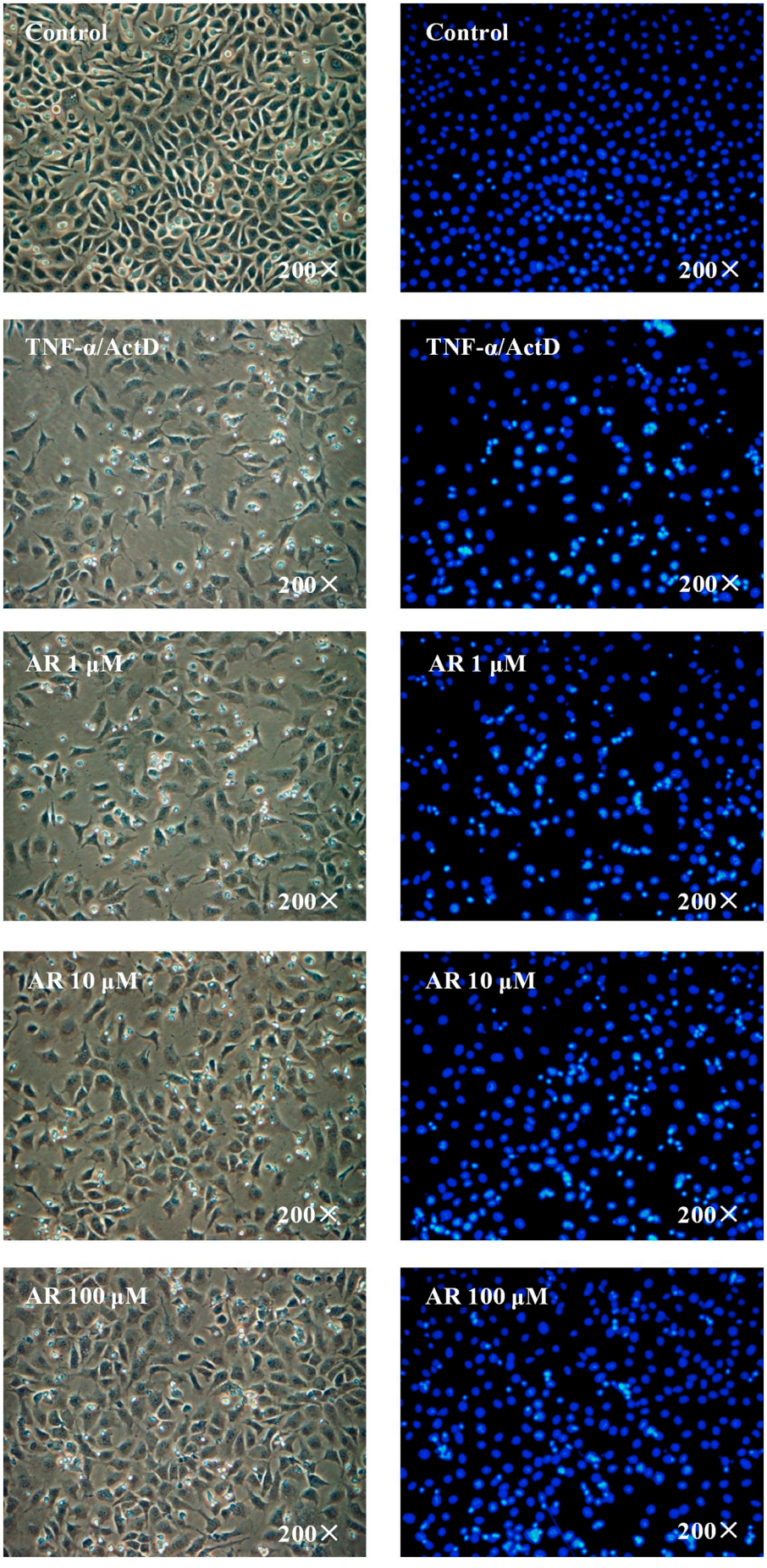

(caption on next page)

Fig. 5. Effects of AR on morphological features of L929 cells exposed to rhTNF-α in the presence of ActD. L929 cells were pretreated with various concentrations of AR (1, 10, and 100 μM) for 1 h in the absence or presence of rhTNF-α/ActD for another 24 h, thereafter stained with Hoechst 33258. The alternations of cellular morphology were observed under phase contrast microscope at 200× magnification, and the nuclear states in the same field of vision were observed under fluorescence microscope. Each representative photograph is out of six independent experiments.

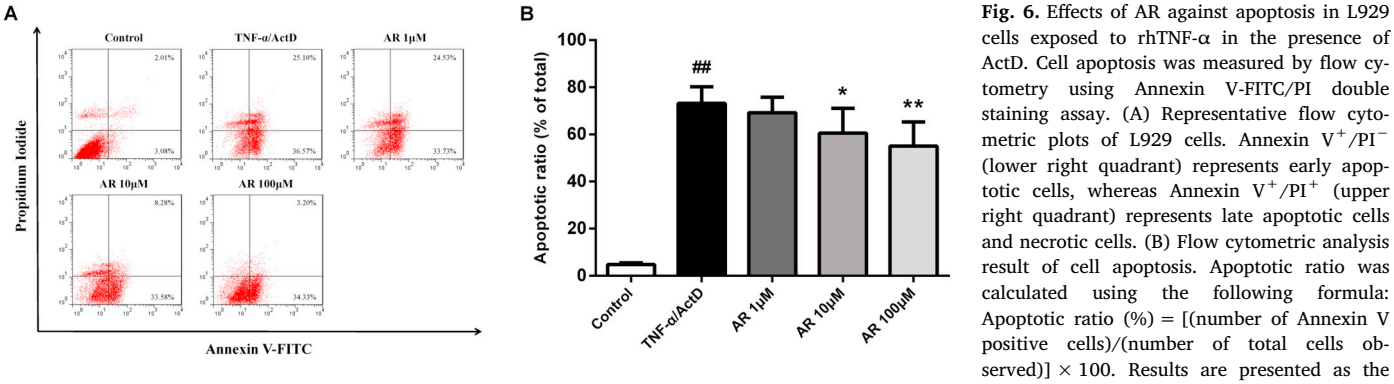

Fig. 6. Effects of AR against apoptosis in L929 cells exposed to rhTNF-α in the presence of ActD. Cell apoptosis was measured by flow cytometry using Annexin V-FITC/PI double staining assay. (A) Representative flow cytometric plots of L929 cells. Annexin V^+/PI^- (lower right quadrant) represents early apoptotic cells, whereas Annexin V^+/PI^+ (upper right quadrant) represents late apoptotic cells and necrotic cells. (B) Flow cytometric analysis result of cell apoptosis. Apoptotic ratio was calculated using the following formula: Apoptotic ratio (%) = [(number of Annexin V positive cells)/(number of total cells observed)] × 100. Results are presented as the mean ± SD of five independent experiments. $^{\#\#}P < 0.01$ versus normal control group; $^{*}P < 0.05$, $^{**}P < 0.01$ versus TNF-α/ActD group.

suppress FLSs mediated synovial inflammation, thus offers potential benefits for RA [32,35–37]. In the present study, the phosphorylation of p38 and ERK was induced apparently upon the stimulation of rhTNF-α in MH7A cell, which was alleviated markedly by AR treatment, indicating that AR might antagonize rhTNF-α-induced responses through down-regulating p38 and ERK MAPK activation.

TNF-α-sensitive murine fibroblast L929 cell line has been successfully used to evaluate various compounds supposed to possess neutralization activity of TNF-α. Hence, this cell model was utilized to investigate the anti-cytotoxic activities of AR against human TNF-α. Our results showed that AR had no significant effect on the viability of L929 cells, suggesting AR has no cytotoxicity at the concentrations tested in vitro (data not shown). Furthermore, our studies indicated that AR conferred protective effects in L929 cells against cytotoxicity induced by rhTNF-α in the presence of ActD, which acts as a transcription inhibitor and sensitizes murine L929 cells to TNF-α-induced cytotoxicity.

Under a phase-contrast and fluorescence microscope, the morphological changes of apoptosis including chromatin condensation and nuclear fragmentation as well as cell shrinkage were observed in L929 cells upon the stimulation of rhTNF-α plus ActD. However, incubation of various concentrations of AR enhanced cell survival, ameliorated cellular damage manifested as the improvement of apoptotic morphologies triggered by rhTNF-α/ActD, indicating that AR could exert protective effects against rhTNF-α-induced cell death. In parallel with the morphological improvement, the Annexin V-FITC/PI double-staining assay demonstrated that the apoptotic ratio triggered by rhTNF-α in the plus of ActD was significantly decreased by AR treatment. It is further supporting the evidence that AR could increase the resistance of L929 cells to rhTNF-α-mediated cytotoxicity.

To gain a better understanding of the protective potential of AR in conferring cellular resistance in response to rhTNF-α, we explored ROS generation and Δψm changes in L929 cells upon the stimulation of rhTNF-α plus ActD. It is well known that the accumulation of ROS above a certain threshold accompanied with impaired mitochondrial function in response to TNF-α could induce cell apoptosis or necrosis [23,38,39]. Mitochondria have been implicated as the rich source of ROS, and damaged mitochondria are facilitated to further release of ROS due to their increased mitochondrial membrane permeability and altered cellular energy production. In turn, sustained and excessive ROS originated from mitochondrial and other intracellular sources induces oxidative stress, eventually leads to mitochondrial function loss and pro-apoptotic transducing molecules release [40–42]. Our results exhibited that excessive ROS production and significant Δψm repression were promoted by the stimulation of rhTNF-α combined with ActD in L929 cells, supporting the notion that cellular oxidative stress as well as mitochondrial dysfunction may contribute to cellular injury. Pretreatment with AR inhibited substantial accumulation of intracellular ROS and prevented the disruption of Δψm, suggesting that AR protects murine L929 cells from rhTNF-α-triggered cell injury probably through the restoration of endogenous antioxidant capacity and improvement of mitochondrial dysfunction.

On the basis of the knowledge that the activities of human TNF-α on murine cell lines were probably mediated by murine TNF-R1 but not

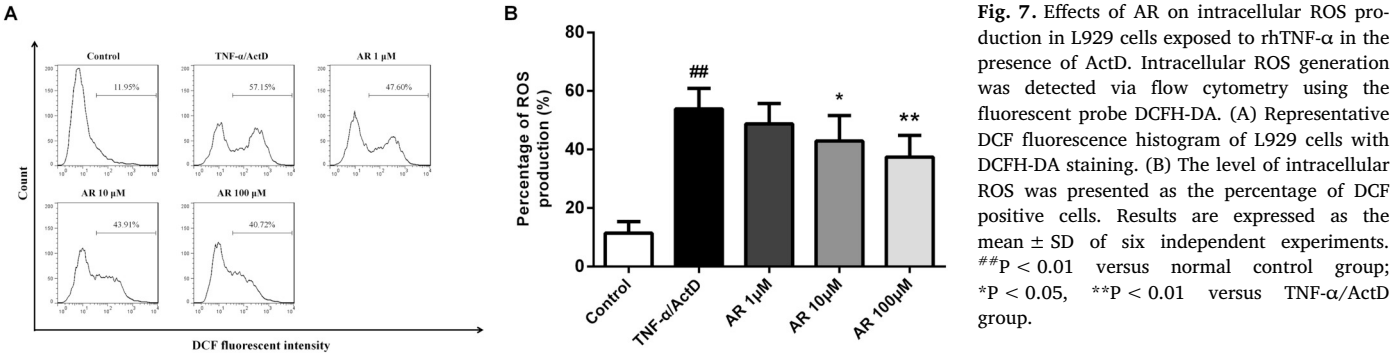

Fig. 7. Effects of AR on intracellular ROS production in L929 cells exposed to rhTNF-α in the presence of ActD. Intracellular ROS generation was detected via flow cytometry using the fluorescent probe DCFH-DA. (A) Representative DCF fluorescence histogram of L929 cells with DCFH-DA staining. (B) The level of intracellular ROS was presented as the percentage of DCF positive cells. Results are expressed as the mean ± SD of six independent experiments. $^{\#\#}P < 0.01$ versus normal control group; $^{*}P < 0.05$, $^{**}P < 0.01$ versus TNF-α/ActD group.

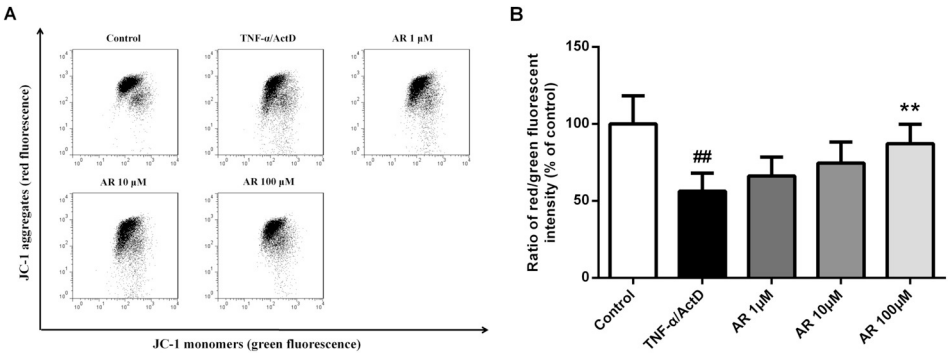

Fig. 8. Effects of AR on mitochondrial membrane potential in L929 cells exposed to rhTNF-α in the presence of ActD. The mitochondrial potential sensor JC-1 was applied, and the ratio of red/green fluorescence intensity was analyzed by flow cytometry. A. Representative flow cytometric fluorescence images of L929 cells with JC-1 staining. B. The ratio of red/green fluorescent intensity was calculated to indicate the ratio of high/low Δψm. The results were presented as the percentage of control group. Values are presented as the mean ± SD of six independent experiments. $^{\#\#}P < 0.01$ versus normal control group; $^{**}P < 0.01$ versus TNF-α/ActD group

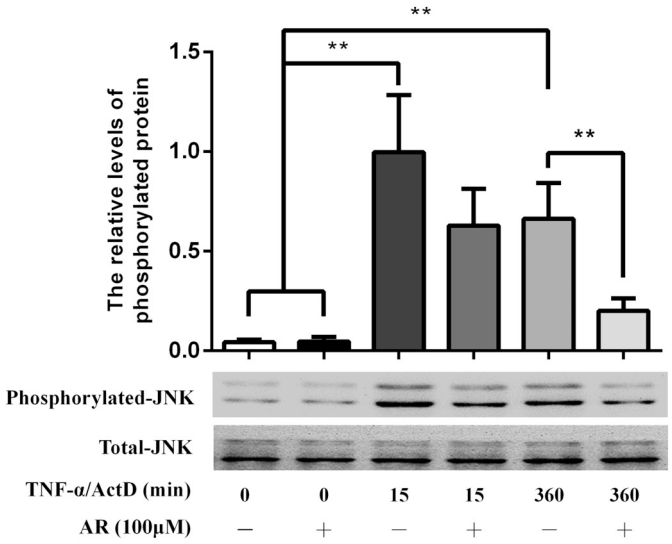

Fig. 9. Effects of AR on the protein levels of JNK phosphorylation in L929 cells exposed to rhTNF-α in the presence of ActD. L929 cells were seeded in 6-well culture plates at a density of 4×10^5 cells/well for 24 h, then incubated in serum-free culture medium for 12 h. Afterwards, the cells were pretreated with 100 μM of AR for 24 h, followed by exposure to TNF-α (5 ng/ml) in the presence of ActD (0.5 μg/ml) for the indicated time, then cell lysates were harvested and subjected to western blotting technique with the indicated antibodies. Lower panel: Representative immunoblots of p-JNK and JNK in L929 cells. Upper panel: Relative band intensities of p-JNK/JNK are shown as the mean ± SD of six independent experiments. $^{**}P < 0.01$.

TNF-R2 [43–45], we speculated that the downstream intracellular signal of TNF-R1 somehow participates in the anti-cytotoxicity of AR against rhTNF-α in murine fibroblast L929 cells. It has been well established that the binding of TNF-α to cell surface TNFR1 leads to the activation of an important stress responsive kinase named as c-Jun N-terminal kinase (JNK) [46,47]. Transient activation of JNK upon TNF-α treatment is associated with cellular survival, whereas prolonged JNK activation contributes to cell death [48,49]. Activation of JNK has been linked to potentiate TNF-α-induced cell death by further enhancing oxidative stress. In turn, TNF-α-induced substantial ROS accumulation promotes sustained activation of JNK [40,46]. As analyzed by western blot, we found that JNK phosphorylated level was enhanced following exposure to rhTNF-α/ActD at 15 min, and the rhTNF-α-triggered TNFR1-JNK activation was sustained until 360 min. The addition of AR to L929 cells resulted in a remarkable decrease of JNK phosphorylation at 360 min, indicating that sustained JNK activation leading to cell death was attenuated by AR pretreatment. Taken together, AR provided protection from cell damage as evidenced by attenuated ROS generation, stabilized mitochondrial membrane potential, and the suppression of sustained JNK activation following rhTNF-α challenge in L929 cells.

In summary, the present study suggested that AR exhibited prominent anti-inflammatory activities in rhTNF-α-stimulated MH7A cells, as well as potent anti-cytotoxic effects in L929 cells upon rhTNF-α stimulation in the presence of ActD. These findings further supported our previous studies and provided new insights on elucidating molecular mechanisms by which AR exerts potent protective properties against inflammation and cytotoxicity triggered by human TNF-α. As the major active component isolated from *Clematis chinensis* Osbeck roots, AR might be a promising alternative candidate for the treatment of rheumatoid arthritis and perhaps other immune-inflammatory diseases in which TNF-α is a key pro-inflammatory mediator.

Conflict of interest statement

The authors declare that there are no conflicts of interest.

Acknowledgments

The work described in this article was supported by the Research Fund for the Doctoral Program of Higher Education (No. 20120096110004), the Doctoral Research Startup Fund of Wannan Medical College (No. rcqd201606), the National Major Scientific and Technological Special Project for "Significant New Drugs Development" during the Thirteenth Five-year Plan Period (No. 2016ZX09101031), and the "Double First-Class" Construction Technology Innovation Team Project of China Pharmaceutical University (No. CPU2018GY23).

References

[1] C. Peng, P.K. Perera, Y.M. Li, W.R. Fang, L.F. Liu, F.W. Li, Anti-inflammatory effects of Clematis chinensis Osbeck extract(AR-6) may be associated with NF-κB, TNF-α, and COX-2 in collagen-induced arthritis in rat, Rheumatol. Int. 32 (10) (2012) 3119–3125.
[2] Li R, Guo LX, Li Y, et al. Dose-response characteristics of Clematis triterpenoid saponins and clematichinenoside AR in rheumatoid arthritis rats by liquid chromatography/mass spectrometry-based serum and urine metabolomics. J. Pharm. Biomed. Anal.. 2017. 136: 81–91.
[3] Han W, Xiong Y, Li Y, et al. Anti-arthritic effects of clematichinenoside (AR-6) on PI3K/Akt signaling pathway and TNF-α associated with collagen-induced arthritis. Pharm. Biol.. 2013. 51(1): 13–22.
[4] S. Hayer, G. Bauer, M. Willburger, et al., Cartilage damage and bone erosion are more prominent determinants of functional impairment in longstanding experimental arthritis than synovial inflammation, Dis. Model. Mech. 9 (11) (2016) 1329–1338.
[5] M. Noack, P. Miossec, Selected cytokine pathways in rheumatoid arthritis, Semin. Immunopathol. 39 (4) (2017) 365–383.
[6] Y. Li, L.M. Wang, J.Z. Xu, K. Tian, C.X. Gu, Z.F. Li, Gastrodia elata attenuates inflammatory response by inhibiting the NF-κB pathway in rheumatoid arthritis fibroblast-like synoviocytes, Biomed. Pharmacother. 85 (2017) 177–181.
[7] K. Klein, P.A. Kabala, A.M. Grabiec, R.E. Gay, C. Kolling, L.L. Lin, et al., The bromodomain protein inhibitor I-BET151 suppresses expression of inflammatory genes and matrix degrading enzymes in rheumatoid arthritis synovial fibroblasts, Ann. Rheum. Dis. 75 (2) (2016) 422–429.
[8] Zeng S, Wang K, Huang M, et al. Halofuginone inhibits TNF-α-induced the migration and proliferation of fibroblast-like synoviocytes from rheumatoid arthritis patients. Int. Immunopharmacol.. 2017. 43: 187–194.
[9] Q. Liang, Y. Ju, Y. Chen, et al., Lymphatic endothelial cells efferent to inflamed joints produce iNOS and inhibit lymphatic vessel contraction and drainage in TNF-induced arthritis in mice, Arthritis Res. Ther. 18 (2016) 62.

[10] A.P. Croft, A.J. Naylor, J.L. Marshall, et al., Rheumatoid synovial fibroblasts differentiate into distinct subsets in the presence of cytokines and cartilage, Arthritis Res. Ther. 18 (1) (2016) 270.
[11] Q. Shi, E.P. Rondon-Cavanzo, I.P. Dalla Picola, M.J. Tiera, X. Zhang, K. Dai, et al., In vivo therapeutic efficacy of TNFα silencing by folate-PEG-chitosan-DEAE/siRNA nanoparticles in arthritic mice, Int. J. Nanomedicine 13 (2018) 387–402.
[12] F. Mirza, J. Lorenzo, H. Drissi, F.Y. Lee, D.Y. Soung, Dried plum alleviates symptoms of inflammatory arthritis in TNF transgenic mice, J. Nutr. Biochem. 52 (2018) 54–61.
[13] Ibrahim F, Lorente-Cánovas B, Doré CJ, et al. Optimizing treatment with tumour necrosis factor inhibitors in rheumatoid arthritis-a proof of principle and exploratory trial: is dose tapering practical in good responders. Rheumatology (Oxford). 2017. 56(11): 2004–2014.
[14] P.A. van Schouwenburg, T. Rispens, G.J. Wolbink, Immunogenicity of anti-TNF biologic therapies for rheumatoid arthritis, Nat. Rev. Rheumatol. 9 (3) (2013) 164–172.
[15] J.R. Kalden, H. Schulze-Koops, Immunogenicity and loss of response to TNF inhibitors: implications for rheumatoid arthritis treatment, Nat. Rev. Rheumatol. 13 (12) (2017) 707–718.
[16] M.S. Prado, K. Bendtzen, A. LEC, Biological anti-TNF drugs: immunogenicity underlying treatment failure and adverse events, Expert Opin. Drug Metab. Toxicol. 13 (9) (2017) 985–995.
[17] S. Minozzi, S. Bonovas, T. Lytras, V. Pecoraro, M. González-Lorenzo, A.J. Bastiampillai, et al., Risk of infections using anti-TNF agents in rheumatoid arthritis, psoriatic arthritis, and ankylosing spondylitis: a systematic review and meta-analysis, Expert Opin Drug Saf 15 (sup1) (2016) 11–34.
[18] Y. Xiong, Y. Ma, W. Han, N.D. Kodithuwakku, L.F. Liu, F.W. Li, et al., Clematichinenoside AR induces immunosuppression involving Treg cells in Peyer's patches of rats with adjuvant induced arthritis, J. Ethnopharmacol. 155 (2) (2014) 1306–1314.
[19] Yan S, Zhang X, Zheng H, et al. Clematichinenoside inhibits VCAM-1 and ICAM-1 expression in TNF-α-treated endothelial cells via NADPH oxidase-dependent IκB kinase/NF-κB pathway. Free Radic. Biol. Med.. 2015. 78: 190–201.
[20] K. Miyazawa, A. Mori, H. Okudaira, Establishment and characterization of a novel human rheumatoid fibroblast-like synoviocyte line, MH7A, immortalized with SV40 T antigen, J. Biochem. 124 (6) (1998) 1153–1162.
[21] Z. Hu, J. Qin, H. Zhang, D. Wang, Y. Hua, J. Ding, et al., Japonicone A antagonizes the activity of TNF-α by directly targeting this cytokine and selectively disrupting its interaction with TNF receptor-1, Biochem. Pharmacol. 84 (11) (2012) 1482–1491.
[22] Y. Cao, Y.H. Li, D.Y. Lv, X.F. Chen, L.D. Chen, Z.Y. Zhu, et al., Identification of a ligand for tumor necrosis factor receptor from Chinese herbs by combination of surface plasmon resonance biosensor and UPLC-MS, Anal. Bioanal. Chem. 408 (19) (2016) 5359–5367.
[23] G. Oláh, K. Módis, D. Gero, et al., Cytoprotective effect of γ-tocopherol against tumor necrosis factor α induced cell dysfunction in L929 cells, Int. J. Mol. Med. 28 (5) (2011) 711–720.
[24] Chang H, Qin W, Li Y, et al. A novel human scFv fragment against TNF-alpha from de novo design method. Mol. Immunol.. 2007. 44(15): 3789–96.
[25] S. Chen, H. Jiang, Y. Cao, Y. Wang, Z. Hu, Z. Zhu, et al., Drug target identification using network analysis: taking active components in Sini decoction as an example, Sci. Rep. 6 (2016) 24245.
[26] M.A. Al-Madol, M. Shaqura, T. John, et al., Comparative expression analyses of pro- versus anti-inflammatory mediators within synovium of patients with joint trauma, osteoarthritis, and rheumatoid arthritis, Mediat. Inflamm. 2017 (2017) 9243736.
[27] I.B. McInnes, C.D. Buckley, J.D. Isaacs, Cytokines in rheumatoid arthritis - shaping the immunological landscape, Nat. Rev. Rheumatol. 12 (1) (2016) 63–68.
[28] J. Li, J. Li, Y. Yue, Y. Hu, W. Cheng, R. Liu, et al., Genistein suppresses tumor necrosis factor α-induced inflammation via modulating reactive oxygen species/Akt/nuclear factor κB and adenosine monophosphate-activated protein kinase signal pathways in human synoviocyte MH7A cells, Drug Des. Devel. Ther. 8 (2014) 315–323.
[29] M. Lao, Z. Zhan, N. Li, S. Xu, M. Shi, Y. Zou, et al., Role of small ubiquitin-like modifier proteins-1 (SUMO-1) in regulating migration and invasion of fibroblast-like synoviocytes from patients with rheumatoid arthritis, Exp. Cell Res. 375 (1) (2019) 52–61.
[30] Y. Araki, T. Mimura, Matrix metalloproteinase gene activation resulting from disordered epigenetic mechanisms in rheumatoid arthritis, Int. J. Mol. Sci. 18 (5) (2017).
[31] E. Kunisch, S. Chakilam, M. Gandesiri, R.W. Kinne, IL-33 regulates TNF-α dependent effects in synovial fibroblasts, Int. J. Mol. Med. 29 (4) (2012) 530–540.
[32] Y. Zou, S. Zeng, M. Huang, Q. Qiu, Y. Xiao, M. Shi, et al., Inhibition of 6-phosphofructo-2-kinase suppresses fibroblast-like synoviocytes-mediated synovial inflammation and joint destruction in rheumatoid arthritis, Br. J. Pharmacol. 174 (9) (2017) 893–908.
[33] B. Görtz, S. Hayer, B. Tuerck, J. Zwerina, J.S. Smolen, G. Schett, Tumour necrosis factor activates the mitogen-activated protein kinases p38alpha and ERK in the synovial membrane in vivo, Arthritis Res. Ther. 7 (5) (2005) R1140–R1147.
[34] E. Kunisch, M. Gandesiri, R. Fuhrmann, A. Roth, R. Winter, R.W. Kinne, Predominant activation of MAP kinases and pro-destructive/pro-inflammatory features by TNF alpha in early-passage synovial fibroblasts via TNF receptor-1: failure of p38 inhibition to suppress matrix metalloproteinase-1 in rheumatoid arthritis, Ann. Rheum. Dis. 66 (8) (2007) 1043–1051.
[35] V.R. Mukaro, A. Quach, M.E. Gahan, B. Boog, Z.H. Huang, X. Gao, et al., Small tumor necrosis factor receptor biologics inhibit the tumor necrosis factor-p38 signalling axis and inflammation, Nat. Commun. 9 (1) (2018) 1365.
[36] S. Namba, R. Nakano, T. Kitanaka, N. Kitanaka, T. Nakayama, H. Sugiya, ERK2 and JNK1 contribute to TNF-α-induced IL-8 expression in synovial fibroblasts, PLoS One 12 (8) (2017) e0182923.
[37] Y.J. Ha, Y.S. Choi, D.W. Han, E.H. Kang, I.S. Yoo, J.H. Kim, et al., PIM-1 kinase is a novel regulator of proinflammatory cytokine-mediated responses in rheumatoid arthritis fibroblast-like synoviocytes, Rheumatology (Oxford) 58 (1) (2019) 154–164.
[38] F. Van Herreweghe, N. Festjens, W. Declercq, P. Vandenabeele, Tumor necrosis factor-mediated cell death: to break or to burst, that's the question, Cell. Mol. Life Sci. 67 (10) (2010) 1567–1579.
[39] M. Xu, C. Cai, X. Sun, W. Chen, Q. Li, H. Zhou, Clnk plays a role in TNF-alpha-induced cell death in murine fibrosarcoma cell line L929, Biochem. Biophys. Res. Commun. 463 (3) (2015) 275–279.
[40] H. Blaser, C. Dostert, T.W. Mak, D. Brenner, TNF and ROS crosstalk in inflammation, Trends Cell Biol. 26 (4) (2016) 249–261.
[41] D.B. Zorov, M. Juhaszova, S.J. Sollott, Mitochondrial reactive oxygen species (ROS) and ROS-induced ROS release, Physiol. Rev. 94 (3) (2014) 909–950.
[42] A. Rimessi, M. Previati, F. Nigro, M.R. Wieckowski, P. Pinton, Mitochondrial reactive oxygen species and inflammation: molecular mechanisms, diseases and promising therapies, Int. J. Biochem. Cell Biol. 81 (Pt B) (2016) 281–293.
[43] M. Lewis, L.A. Tartaglia, A. Lee, et al., Cloning and expression of cDNAs for two distinct murine tumor necrosis factor receptors demonstrate one receptor is species specific, Proc. Natl. Acad. Sci. U. S. A. 88 (7) (1991) 2830–2834.
[44] L.A. Tartaglia, R.F. Weber, I.S. Figari, C. Reynolds, M.A. Palladino, D.V. Goeddel, The two different receptors for tumor necrosis factor mediate distinct cellular responses, Proc. Natl. Acad. Sci. U. S. A. 88 (20) (1991) 9292–9296.
[45] F. Mackay, J. Rothe, H. Bluethmann, H. Loetscher, W. Lesslauer, Differential responses of fibroblasts from wild-type and TNF-R55-deficient mice to mouse and human TNF-alpha activation, J. Immunol. 153 (11) (1994) 5274–5284.
[46] M.J. Morgan, Z.G. Liu, Reactive oxygen species in TNFalpha-induced signaling and cell death, Mol. Cell 30 (1) (2010) 1–12.
[47] S. Saveljeva, L.S.L. Mc, P. Vandenabeele, A. Samali, M.J. Bertrand, Endoplasmic reticulum stress induces ligand-independent TNFR1-mediated necroptosis in L929 cells, Cell Death Dis. 6 (2015) e1587.
[48] A. Wullaert, K. Heyninck, R. Beyaert, Mechanisms of crosstalk between TNF-induced NF-kappaB and JNK activation in hepatocytes, Biochem. Pharmacol. 72 (9) (2006) 1090–1101.
[49] D. Wang, M. Zhao, G. Chen, X. Cheng, X. Han, S. Lin, et al., The histone deacetylase inhibitor vorinostat prevents TNFα-induced necroptosis by regulating multiple signaling pathways, Apoptosis 18 (11) (2013) 1348–1362.